Supporting Information for

Two-Photon Spectroscopy of the Q-Bands of *meso*-Tetraphenyl-Porphyrin and -Chlorin Framework Derivatives

Jordan A. Greco,[†] Sumie Shima,[†] Nicole L. Wagner,[‡] Jason R. McCarthy,[†] Karissa Atticks,[†] Christian Brückner,[,†] and Robert R. Birge*[,†,‡]*

[†]Department of Chemistry, University of Connecticut, 55 North Eagleville Road, Storrs, Connecticut 06269-3060, United States.

[‡]Department of Molecular and Cell Biology, University of Connecticut, 91 North Eagleville Road, Storrs, Connecticut 06269-3125, United States.

Table of Contents:

Table S1. Two-photon absorptivities of rhodamine B in methanol and 95:5 CS_2:methanol (v/v) in the 900 – 1200 nm region.

Table S2. Vibronic analysis of the $S_0 \rightarrow S_1(Q_x)$ transition of porphin.

Table S3. Vibronic analysis of the $S_0 \rightarrow S_1(Q_x)$ transition of chlorin.

Table S4. Normal-coordinate structure decomposition (NSD) of the out-of-plane distortions of **(OMe)$_2$TPC**.

Figure S1. Regression analysis of the multi-photon excitation of **TPP** at 1200 nm.

Figure S2. An alternative approach to the graphical validation of the two-photon character of the signals observed from two-photon excitation of **TPP** at 1200 nm observed by plotting the signal intensity versus the square of the laser excitation energy.

Figure S3. Two-photon excitation spectra of rhodamine B in CS_2 with 5% methanol (v/v) and pure methanol.

Figure S4. Decomposition of the oscillator strength of the Q_x and Q_y bands of porphin and **TPP** in CS_2.

Figure S5. Decomposition of the oscillator strength of the Q_y and Q_x bands of the three tetraphenyl-chlorins in CS_2.

Figure S6. Analysis of the maximum in the line shape function, g_{max}, for porphin and **TPP**.

Figure S7. Analysis of the maximum in the line shape function, g_{max}, for the three chlorin-like porphyrinoids studied in this paper.

Table S1. Two-Photon Absorptivities[a] (TPA) of Rhodamine B in MeOH and 95:5 CS_2:MeOH (v/v) in the 900 – 1200 nm Region

wavelength (nm)	TPA(GM) (MeOH)	TPA(GM) (CS_2/MeOH)
900	3.85 ± 0.59	3.86 ± 0.66
910	4.28 ± 0.78	3.39 ± 0.64
920	6.13 ± 0.96	3.64 ± 0.54
930	7.53 ± 1.09	4.03 ± 0.63
940	9.44 ± 1.70	4.59 ± 0.73
950	11.30 ± 1.88	5.69 ± 0.93
960	12.75 ± 2.20	6.55 ± 0.97
970	15.44 ± 2.39	7.90 ± 1.21
980	18.06 ± 2.94	9.73 ± 1.39
990	22.20 ± 3.43	11.15 ± 2.29
1000	26.41 ± 4.82	12.92 ± 2.35
1010	29.21 ± 4.96	15.76 ± 2.98
1020	31.87 ± 5.96	18.93 ± 3.37
1030	32.45 ± 5.70	22.23 ± 3.64
1040	32.55 ± 4.27	25.56 ± 3.78
1050	34.34 ± 5.39	27.66 ± 4.21
1060	36.71 ± 5.01	28.07 ± 3.91
1070	40.87 ± 6.18	28.33 ± 4.68
1080	44.63 ± 6.84	29.93 ± 4.23
1090	43.00 ± 7.24	33.11 ± 5.82
1100	35.98 ± 5.19	37.70 ± 7.37
1110	25.86 ± 5.09	42.82 ± 6.64
1120	16.35 ± 2.70	46.18 ± 9.29
1130	9.47 ± 1.86	44.79 ± 7.70
1140	4.93 ± 0.97	37.34 ± 4.38
1150	2.28 ± 0.40	26.31 ± 4.08
1160	0.93 ± 0.15	15.95 ± 2.43
1170	0.34 ± 0.08	8.53 ± 1.24
1180	0.13 ± 0.02	4.06 ± 0.66
1190	0.05 ± 0.01	1.73 ± 0.34
1200	0.02 ± 0.01	0.71 ± 0.22

[a]Two-photon absorptivities for two parallel propagating photons of identical energy and polarization. Values in units of Göppert-Mayers (1 GM = 10^{-50} cm^4 s).

Table S2. Vibronic Analysis of the $S_0 \rightarrow S_1(Q_x)$ Transition of Porphin[a]

#(0)	#(*)	freq(0)	freq(*)	sym	IR(0)	IR(*)	force(0)	force(*)	rmass(0)	rmass(*)	Δfreq	ΔQ
77	76	1508.773	1496.31	a_g	0	0	13.00	9.366	9.697	7.100	-12.456	0.0421
81	80	1559.936	1544.04	a_g	0	0	4.292	4.964	2.994	3.534	-15.891	0.0249
84	83	1608.509	1589.56	a_g	0	0	9.639	7.832	6.323	5.261	-18.942	0.0288
3	2	75.696	73.798	a_u	0	0	0.017	0.016	5.112	5.115	-1.898	0.0558
13	11	329.366	316.503	a_u	0	0	0.299	0.281	4.682	4.758	-12.863	0.0274
23	22	526.170	493.527	a_u	0	0	0.615	0.537	3.769	3.741	-32.643	0.0465
29	27	753.404	736.361	a_u	0	0	1.505	1.327	4.501	4.153	-17.043	0.0321
30	28	775.727	753.611	a_u	0	0	1.249	1.157	3.522	3.456	-22.116	0.0206
7	6	143.625	136.900	b_{1g}	0	0	0.064	0.058	5.221	5.243	-6.725	0.0666
10	10	226.437	219.952	b_{1g}	0	0	0.172	0.165	5.692	5.77	-6.485	0.023
22	21	484.817	451.525	b_{1g}	0	0	0.534	0.46	3.856	3.833	-33.292	0.0534
40	39	885.379	869.223	b_{1g}	0	0	0.777	0.686	1.683	1.541	-16.156	0.0396
6	5	138.804	130.417	b_{2g}	0	0	0.048	0.043	4.239	4.297	-8.387	0.0887
9	8	206.535	200.719	b_{2g}	0	0	0.129	0.123	5.123	5.192	-5.816	0.0249
21	19	469.239	437.042	b_{2g}	0	0	0.496	0.429	3.824	3.815	-32.197	0.0533
25	23	713.094	679.435	b_{2g}	0	0	0.381	0.353	1.272	1.298	-33.659	0.0305
27	25	733.969	722.831	b_{2g}	0	0	0.822	0.775	2.590	2.517	-11.138	0.0182
32	30	783.595	760.052	b_{2g}	0	0	1.249	1.152	3.452	3.385	-23.543	0.0216
44	41	890.565	870.425	b_{2g}	0	0	0.648	0.605	1.387	1.354	-20.140	0.0233
73	71	1400.042	1373.66	b_{3g}	0	0	1.753	2.048	1.518	1.842	-26.375	0.0358
76	74	1482.869	1480.83	b_{3g}	0	0	4.679	3.340	3.611	2.585	-2.039	0.0608
78	77	1522.234	1510.58	b_{3g}	0	0	2.706	3.154	1.982	2.346	-11.645	0.0306
79	78	1551.624	1524.81	b_{3g}	0	0	5.225	3.243	3.684	2.368	-26.809	0.0849
94	91	1772.172	1739.15	b_{3g}	0	0	8.419	7.033	4.55	3.946	-33.014	0.0260
85	84	1655.378	1618.26	b_{1u}	0	4	8.365	7.001	5.181	4.537	-37.109	0.0258
90	88	1706.592	1687.53	b_{1u}	7	12	7.970	7.152	4.644	4.263	-19.061	0.0157
24	36	650.805	808.15	b_{2u}	526	34	2.074	1.888	8.309	4.907	157.345	0.0213
38	37	830.403	847.279	b_{2u}	1	0	1.919	2.492	4.723	5.891	16.876	0.0574
45	49	893.362	1008.10	b_{2u}	103	148	2.153	4.134	4.579	6.905	114.743	0.1294
57	57	1075.839	1076.38	b_{2u}	11	3	2.469	1.804	3.621	2.643	0.544	0.0698
62	61	1145.778	1172.97	b_{2u}	14	26	1.633	0.965	2.111	1.19	27.198	0.1393
66	67	1217.36	1281.72	b_{2u}	1	2	1.319	1.780	1.511	1.839	64.368	0.0741
69	68	1295.702	1303.63	b_{2u}	1	2	1.545	2.495	1.562	2.492	7.935	0.1092
72	72	1387.969	1377.42	b_{2u}	40	30	3.080	3.255	2.713	2.911	-10.548	0.0107
75	75	1476.992	1487.57	b_{2u}	1	0	1.817	2.139	1.414	1.64	10.579	0.0370
83	82	1595.380	1579.90	b_{2u}	18	25	5.108	4.612	3.406	3.136	-15.476	0.0172
86	85	1666.160	1666.35	b_{2u}	2	1	4.893	5.253	2.992	3.211	0.196	0.0118
89	89	1694.563	1687.77	b_{2u}	0	4	10.47	8.571	6.192	5.107	-6.787	0.0270
2	1	61.018	58.058	b_{3u}	0	0	0.012	0.011	5.639	5.591	-2.960	0.1355
11	9	227.252	215.051	b_{3u}	3	2	0.214	0.198	7.021	7.282	-12.201	0.0357
16	15	368.649	343.601	b_{3u}	7	7	0.305	0.265	3.804	3.816	-25.048	0.0596
26	24	720.593	701.603	b_{3u}	1	4	1.015	0.942	3.318	3.247	-18.99	0.0216
42	40	888.514	869.307	b_{3u}	179	186	0.722	0.602	1.552	1.352	-19.207	0.0595

[a]Only vibronic modes involving ΔQ>0.02 are listed. The ground [freq(0)] and excited singlet [freq(*)] state vibrational frequencies are in wavenumbers (cm^{-1}), the IR intensities of the modes for the ground [IR(0)] and excited singlet [IR(*)] states are in KM/mol, the ground [force(0)] and excited singlet [force(*)] state force constants are listed in mDyne/Å, and the ground [rmass(0)] and excited singlet [rmass(*)] state force constants are listed in amu. The change in frequency, Δfreq, is in wavenumbers (cm^{-1}) and the dimensionless coordinate displacement, ΔQ, is listed in the last column.

Table S3. Vibronic Analysis of the $S_0 \rightarrow S_1(Q_y)$ Transition of Chlorin[a]

#(0)	#(*)	freq(0)	freq(*)	sym	IR(0)	IR(*)	force(0)	force(*)	rmass(0)	rmass(*)	$\Delta\sigma/cm^{-1}$	ΔQ
13	12	319.837	322.595	a_1	1	0	0.310	0.323	5.139	5.272	2.758	0.017
79	81	1498.695	1515.603	a_1	46	6	3.011	3.675	2.276	2.716	7.289	0.035
86	91	1580.632	1661.108	a_1	0	83	8.808	6.091	5.984	3.747	11.777	0.050
88	85	1623.596	1584.717	a_1	81	7	4.033	5.939	2.597	4.014	4.085	0.060
89	89	1642.092	1641.477	a_1	54	0	2.128	1.788	1.339	1.127	-0.615	0.037
90	84	1649.331	1541.277	a_1	187	1	3.998	4.996	2.495	3.570	-7.492	0.036
7	6	133.623	129.597	a_2	0	0	0.044	0.042	4.217	4.227	-4.026	0.044
17	16	359.221	348.927	a_2	0	0	0.344	0.324	4.518	4.522	-10.294	0.022
23	22	516.697	472.219	a_2	0	0	0.570	0.496	3.626	3.778	-44.478	0.045
24	27	623.071	715.501	a_2	0	0	0.778	0.942	3.401	3.122	10.560	0.053
27	25	698.960	669.565	a_2	0	0	0.505	0.325	1.753	1.232	-29.395	0.157
28	23	704.941	593.064	a_2	0	0	0.529	0.683	1.806	3.296	-30.007	0.080
46	47	917.505	946.128	a_2	0	0	0.808	0.729	1.629	1.382	-47.106	0.030
49	45	993.234	899.599	a_2	0	0	0.743	0.689	1.277	1.446	-17.906	0.022
53	52	1056.036	1032.688	a_2	0	0	0.919	0.864	1.399	1.375	-23.348	0.017
3	2	55.524	53.908	b_1	0	0	0.009	0.009	5.061	5.053	-1.616	0.078
5	4	100.512	99.641	b_1	10	10	0.025	0.024	4.167	4.166	-0.871	0.016
10	9	216.427	213.387	b_1	2	1	0.172	0.163	6.226	6.086	-3.040	0.025
16	13	340.770	322.804	b_1	5	4	0.266	0.242	3.888	3.949	-17.966	0.039
22	20	477.974	437.318	b_1	1	0	0.502	0.437	3.727	3.879	-40.656	0.047
26	29	696.999	751.135	b_1	1	0	1.168	1.065	4.082	3.202	-26.879	0.024
36	33	809.112	782.875	b_1	52	74	0.462	0.437	1.198	1.210	-26.237	0.019
41	40	864.978	856.203	b_1	4	42	0.545	0.520	1.236	1.204	-8.775	0.015
45	42	904.397	868.677	b_1	59	67	0.728	0.686	1.510	1.542	-0.466	0.018
47	49	931.727	955.185	b_1	191	142	0.822	0.774	1.606	1.441	-62.116	0.017
50	46	1017.301	919.647	b_1	34	78	0.805	0.743	1.320	1.491	-12.080	0.023
54	51	1056.449	1012.852	b_1	11	3	0.915	0.837	1.392	1.385	-43.597	0.025
15	15	337.412	332.275	b_2	0	0	0.451	0.429	6.719	6.595	-5.137	0.017
67	70	1279.701	1307.550	b_2	38	2	1.563	1.831	1.620	1.818	-12.789	0.035
70	71	1308.696	1330.855	b_2	67	130	2.089	2.484	2.070	2.381	-69.505	0.035
71	65	1320.339	1260.854	b_2	2	2	1.746	1.986	1.699	2.120	-18.847	0.028
75	68	1400.360	1290.719	b_2	157	138	1.759	2.324	1.522	2.368	-17.977	0.058
77	78	1419.289	1487.972	b_2	4	18	2.666	2.466	2.246	1.890	-23.450	0.015
78	77	1465.802	1420.643	b_2	602	8	3.658	2.662	2.889	2.239	-45.159	0.058
81	76	1511.422	1415.417	b_2	558	42	3.597	2.497	2.672	2.115	-3.872	0.067
82	80	1536.433	1509.640	b_2	3	0	4.378	3.473	3.147	2.586	-26.793	0.039
84	88	1552.389	1617.052	b_2	25	53	4.082	3.092	2.875	2.007	-33.033	0.048
85	82	1578.007	1530.389	b_2	23	35	5.002	3.731	3.409	2.704	-22.000	0.048
87	86	1612.806	1607.704	b_2	0	43	1.679	2.172	1.096	1.427	-5.102	0.055
93	90	1693.031	1644.822	b_2	36	31	6.578	5.302	3.895	3.326	-48.209	0.032
94	103	1741.194	3368.485	b_2	396	10	11.214	7.284	6.278	1.089	1.742	0.055
98	95	1796.583	1736.557	b_2	548	2	10.011	7.203	5.264	4.054	-60.026	0.043

[a]Only vibronic modes involving $\Delta Q>0.014$ are listed. Other details as in Table S2.

Table S4. Normal-Coordinate Structure Decomposition (NSD)[a] of the Out-of-Plane Distortions of **$(OMe)_2$TPC**[b]

molecule	B_{2u}	B_{1u}	A_{2u}	$E_g(x)$	$E_g(y)$	A_{1u}
$(OMe)_2$TPC (DFT)	-0.6194	-0.3918	0.0137	0.0193	0.0848	0.1209
$(OMe)_2$TPC (PM3)	-1.8062	-0.1599	-0.1199	0.1577	-0.511	-0.0023

[a]The NSD analysis is based on methods developed in references 85 and 86.

[b]The absolute value of each quantity is proportional to the out-of-plane distortion. The sign is only dependent on the orientation of the molecule and has no impact on the extent of distortion.

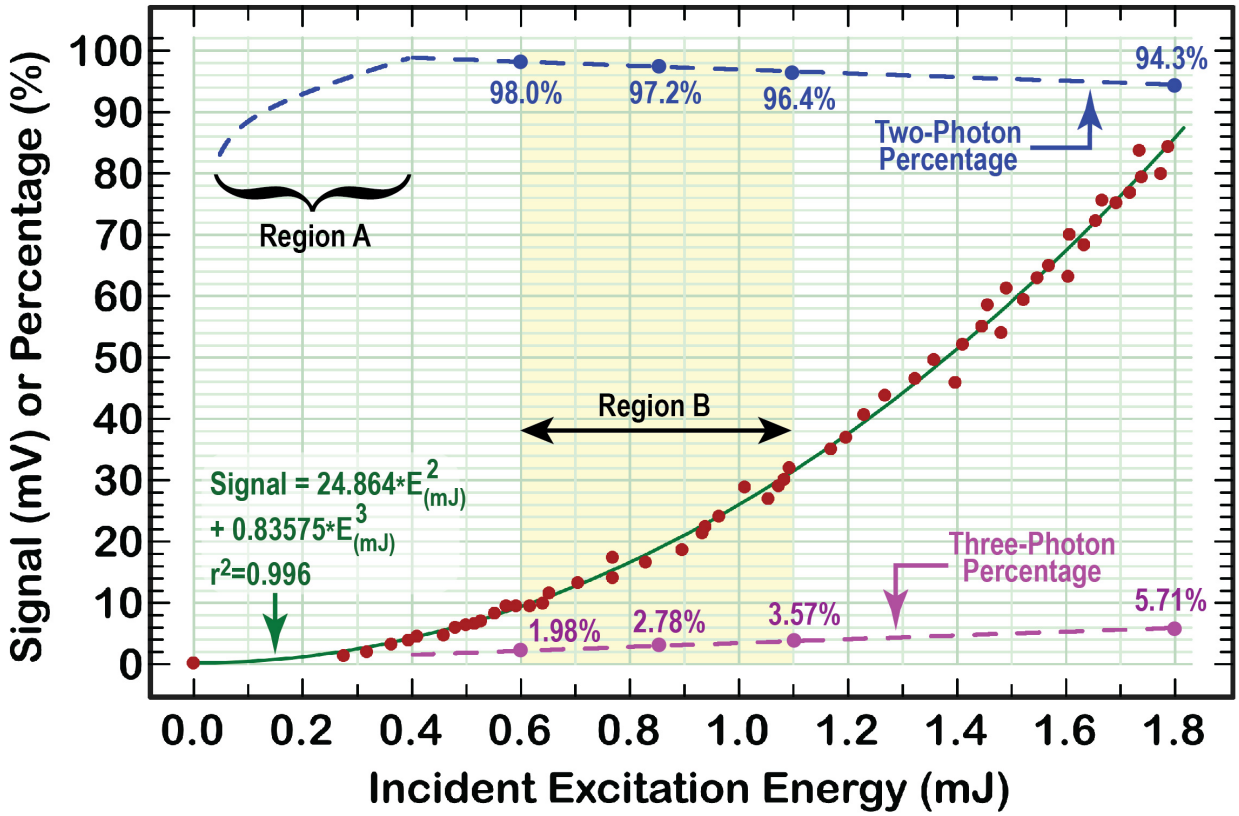

Figure S1. Regression analysis of the laser induced fluorescence of **TPP** at 1200 nm excitation. The equation Signal = a*E^m + b*E^n, where m and n are constrained to be unique integers, was fit to the data by using singular value decomposition and yielded the equation and fit shown in green. Fits to higher order equations such as a*E^l + b*E^m + c*E^n generated worse fits based on minimization of RMS error times parameters. We are thus confident that within experimental error, our data show evidence of only two-photon and three-photon excitation processes. Our spectra were collected using energies in **Region B** to maximize the percentage of two-photon signal while avoiding **Region A**, in which one-photon events have a significant impact on the signal. Although multi-photon processes should be fit with respect to intensity rather than energy, we used the incident energy because it was a directly measured quantity (see Figure 3). The pulse width is invariant to energy in these experiments, and thus the incident intensity is linearly proportional to the energy. The 1200 nm excitation wavelength excites near the maximum of the second vibronic band of **TPP**, assuming a two-photon process. The final state excitation wavenumber is indicated by using a green arrow in Figure S4.

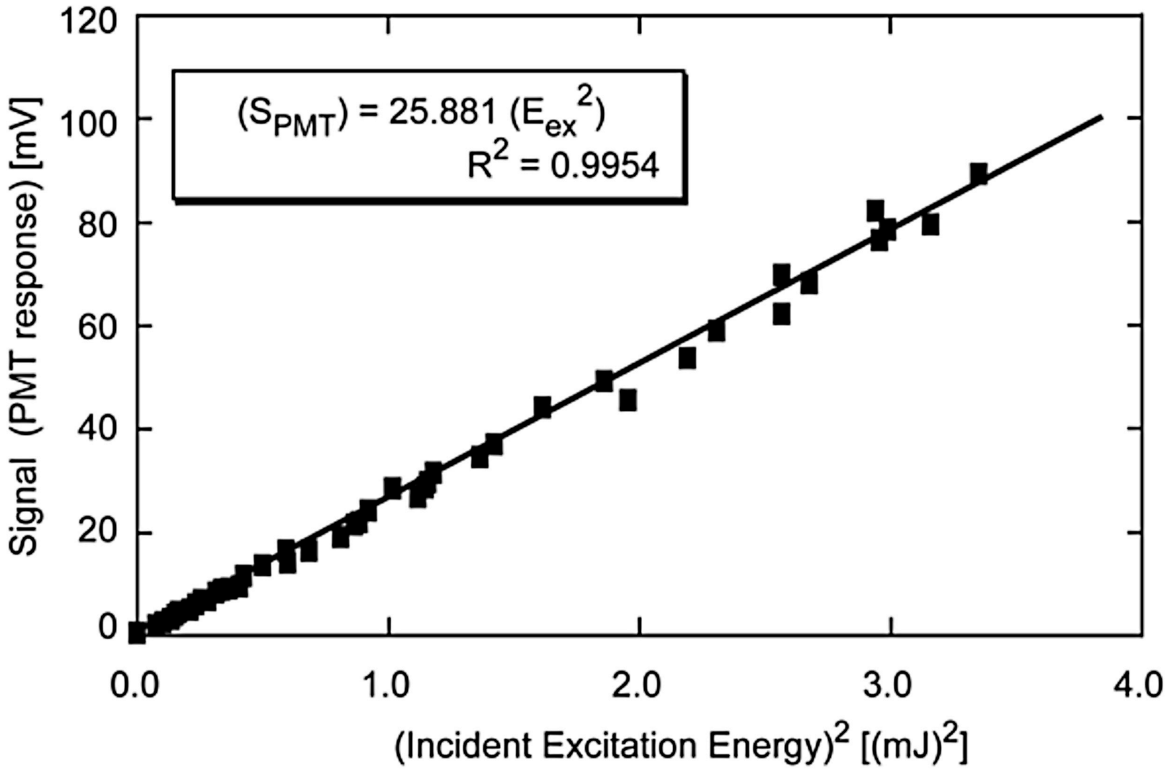

Figure S2. An alternative approach to the graphical validation of the two-photon character of the signals observed from two-photon excitation of **TPP** at 1200 nm observed by plotting the signal intensity versus the square of the laser excitation energy.

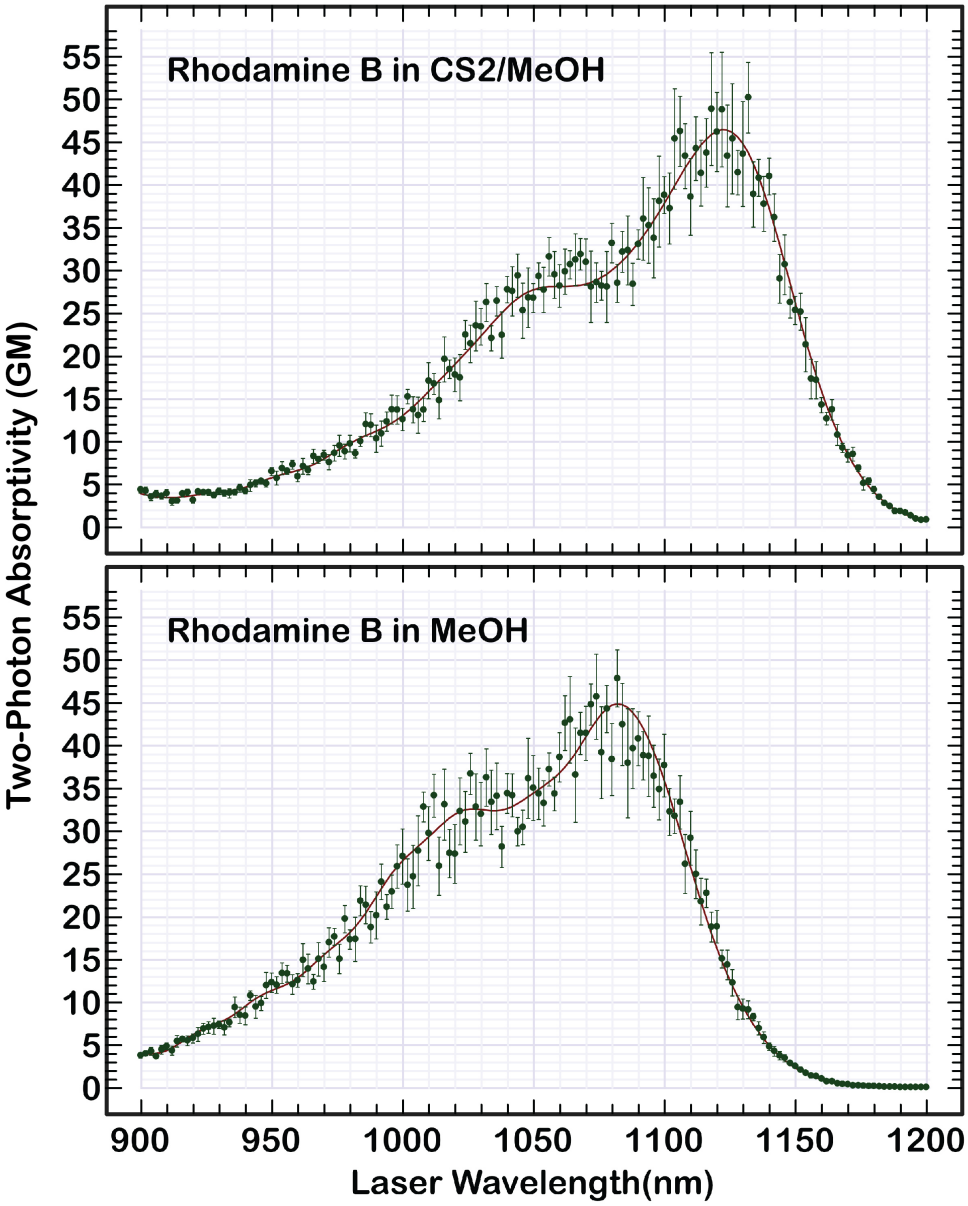

Figure S3. Two-photon excitation spectra of rhodamine B in CS_2 with 5% methanol (v/v) (top) and pure methanol (bottom). The vertical axis is in units of Göppert-Mayers (1 GM = 10^{-50} cm^4 s). The observed absorptivities, averaged in increments of 10 nm, are listed in Table S1.

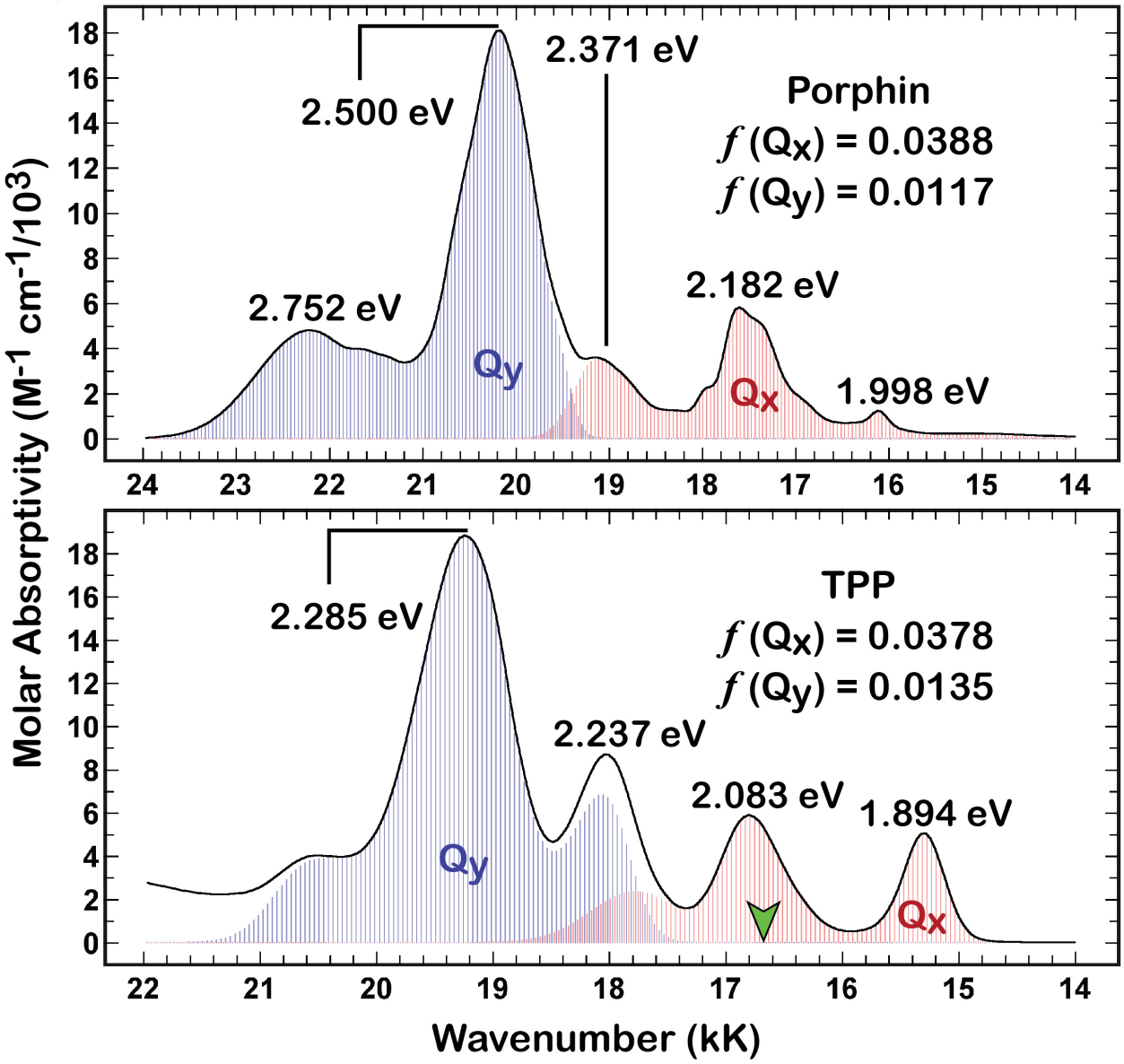

Figure S4. Decomposition of the oscillator strength of the Q_x and Q_y bands of porphin (top) and **TPP** (bottom) in CS_2. The experimental spectra were fit to multiple Gaussian bands and the bands were partitioned into the Q_x and Q_y bands by inspection. The oscillator strength was calculated by summing the oscillator strengths associated with the component Gaussians (see text). The first and maximum vibronic band maxima are assigned in electron volts (eV). The green arrow indicates the final excitation wavenumber, which was determined via the analysis shown in Figure S1.

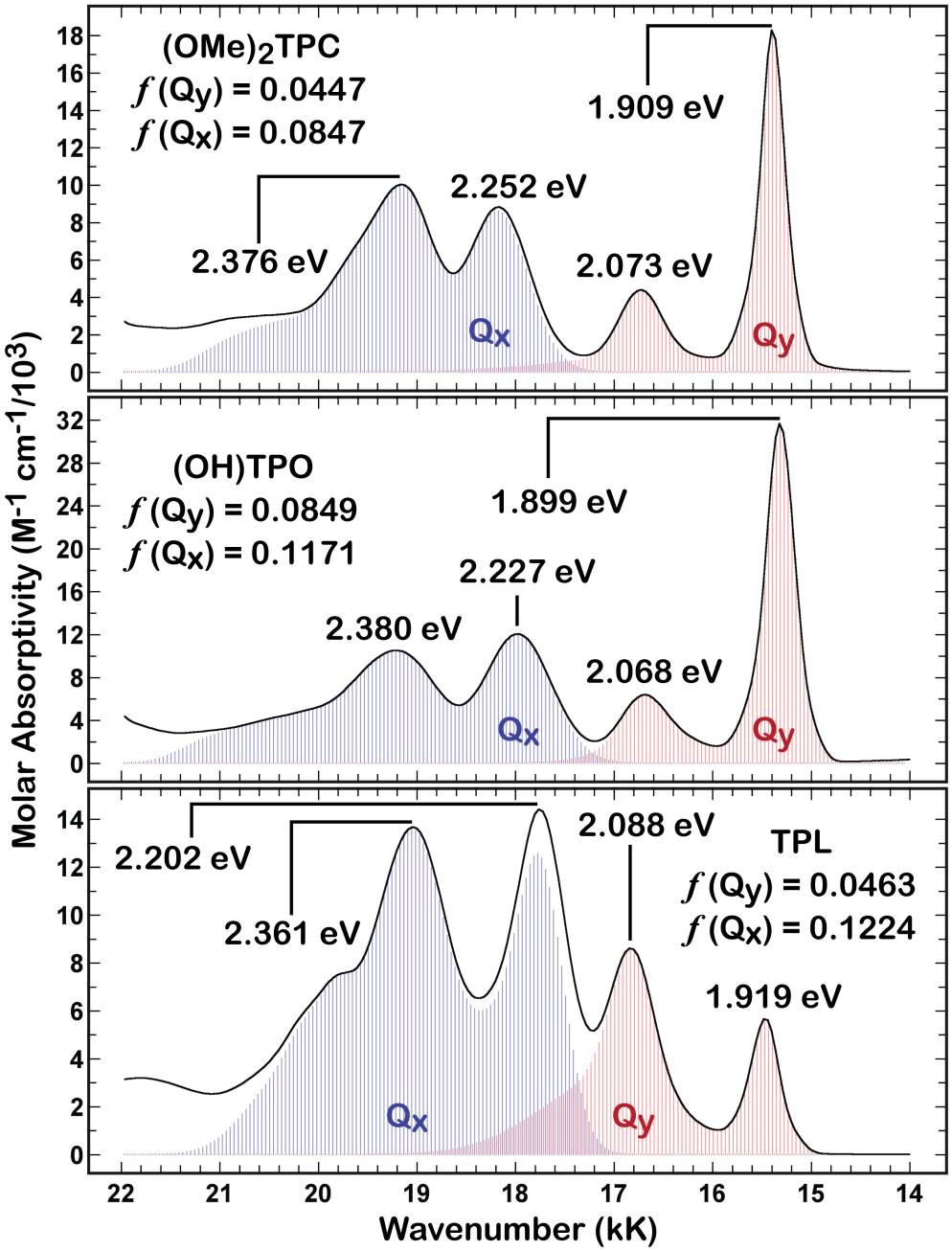

Figure S5. Decomposition of the oscillator strength of the Q_y and Q_x bands of three chlorin-like porphyrinoids in CS_2. See the caption for Figure S4 for further details.

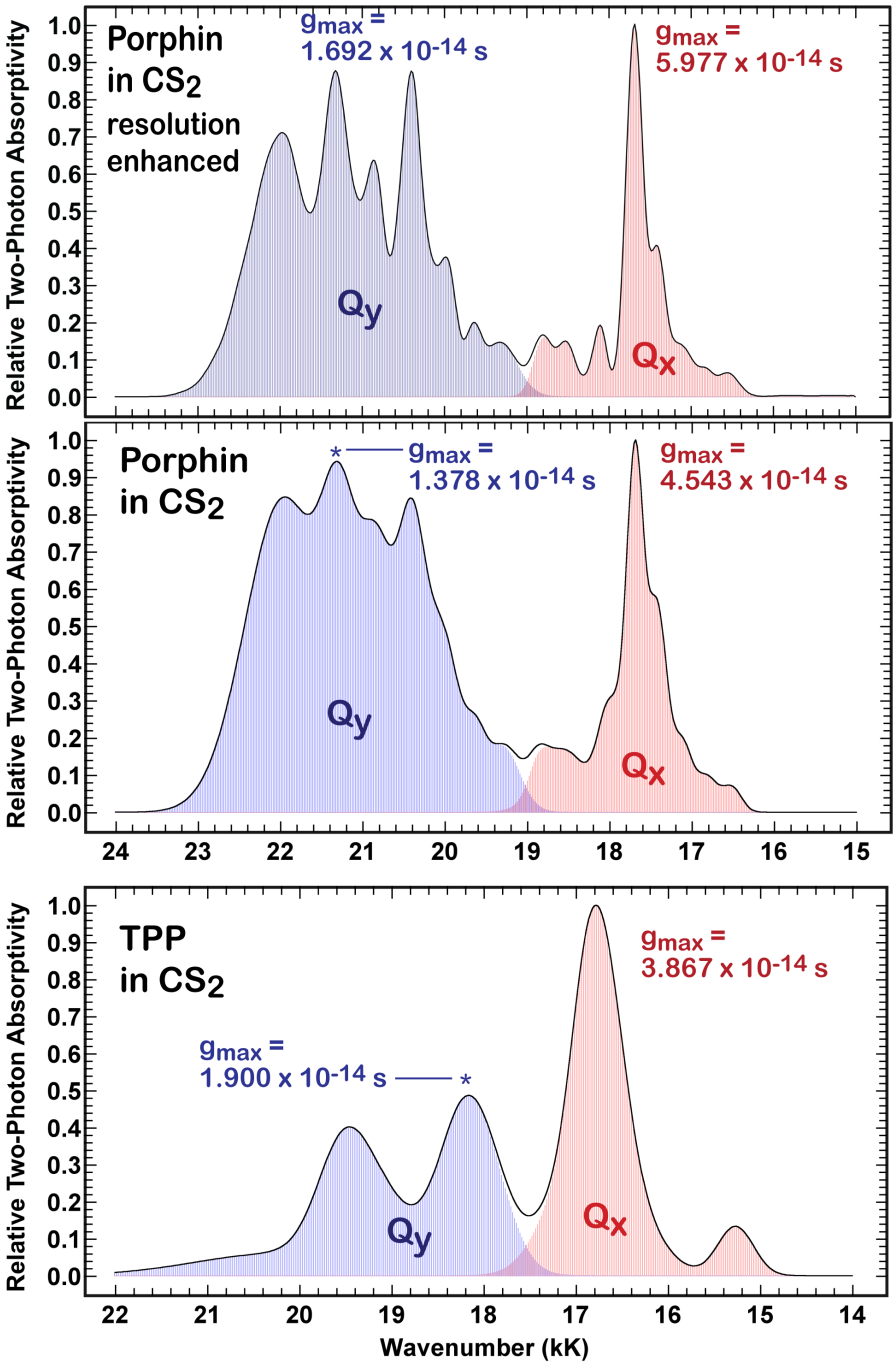

Figure S6. Analysis of the maximum in the line shape function, g_{max}, for porphin (top) and **TPP** (bottom). The observed two-photon spectra were fit using Gaussian bands and the component bands were assigned to the Q_x and Q_y bands via inspection. The normalized bands were integrated over frequency and the inverse of the integral yields g_{max}. The top spectrum used resolution enhancement to explore the impact of resolution on g_{max}. Note that as the vibronic features become sharper, the value of g_{max} increases accordingly.

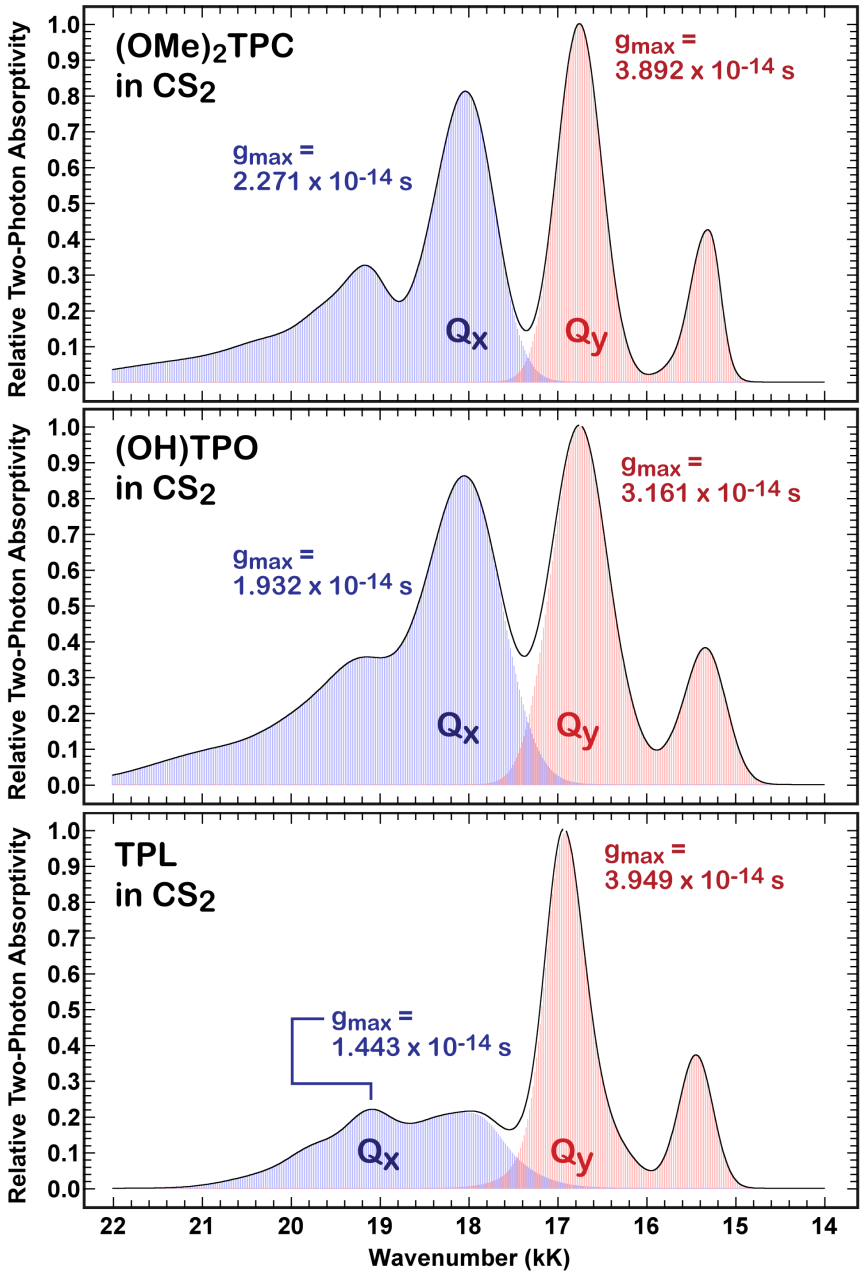

Figure S7. Analysis of the maximum in the line shape function, g_{max}, for **(OMe)$_2$TPC**, **(OH)TPO**, and **TPL**. Other details as in Figure S6.